Adaptive Control of the Nitrate Level in an Activated Sludge Process Using an External Carbon Source - Extended Version

M. Ekman, P. Samuelsson and B. Carlsson

Department of Information Technology
Uppsala University
Box 337, SE-751 05 Uppsala, Sweden

Technical report 2003-030
May 2003
ISSN 1404-3203

Adaptive Control of the Nitrate Level in an Activated Sludge Process Using an External Carbon Source - Extended Version

M. Ekman, P. Samuelsson and B. Carlsson

Department of Information Technology
Division of Systems and Control
Uppsala University
Sweden

July 29, 2003

Abstract

In an activated sludge process for nitrogen removal, nitrate may be reduced to nitrogen gas by facultative heterotrophic bacteria in an anoxic environment. In order to guarantee sufficient supplies of readily biodegradable carbon compounds, an external carbon source often needs to be added. In this report, we present an automatic control strategy for controlling the nitrate level using an external carbon source. The external carbon source is added in the first anoxic compartment and the nitrate concentration in the last anoxic compartment is controlled. Key process parameters of a simplified Activated Sludge Model No. 1 are estimated on-line. The estimated parameters are used for updating the parameters of a linear quadratic controller. The strategy is illustrated in a simulation study using realistic influent data and is shown to perform well.

Contents

1 Introduction

The activated sludge process (ASP) is a commonly used concept for processing biological nitrogen removal in municipal wastewater treatment plants (WWTP's). The degree of nitrogen removal in an ASP is dependent on the efficiency of two biological processes; nitrification and denitrification. By nitrification ammonium is oxidized to nitrate and in the denitrification nitrate is transformed to nitrogen gas. Nitrate can be reduced to nitrogen gas by faculatative heterotrophic bacteria in an anoxic environment. An organic carbon source is needed as electron donor and to supply carbon for synthesis of cell components. If the Carbon/Nitrate ratio is too low in the influent water to the anoxic zone, an addition of external carbon source is required [14]. An important question is how much carbon that should be added. A too high carbon dosage is expensive, may increase the BOD level in the effluent, increase the sludge production [2] and decrease the capacity of the microorganisms to use naturally existing carbon sources [12]. On the other hand, a too low carbon dosage will leave the denitrification process carbon constrained, and the full capacity for nitrogen removal is not utilized.

Adaptive and model-based approaches for control and estimation of wastewater treatment plants have been frequently reported in the literature. Such an approach is, for example, found in [5]. The IWA Activated Sludge Model No.1 (ASM1) described in [13] is frequently used for modeling of ASP's. [15] and [27] discuss the need for model reduction and different reduction approaches for the ASM1 when model based control strategies are suggested. In [18] an adaptive MPC evaluated on an alternating ASP, with dissolved oxygen concentration as control input and ammonium and nitrate concentrations as controlled outputs, is presented. The reduced order model used in the control design is based upon ASM1, see [19]. In [16] several different controllers for a predenitrifying process are designed.

Some of the reported strategies consider control of the nitrate concentration using the external carbon dosage as an input signal. In [17] a direct adaptive strategy for controlling the nitrate concentration, based on a generalized minimum-variance (GMV) strategy, is evaluated in a predenitrifying pilot plant. A controller design based on the ASM1 is presented in [29]. The choice of setpoint for the carbon controller is also considered. A feedforward strategy based on a simple mass balance is presented in [23]. A related strategy can be found in [6] where a model based feedback-feedforward controller is designed using exact linearization on a simplified ASM1. A cascade control strategy for controlling the nitrate concentration in both the effluent and in the last anoxic compartment is proposed in [7].

In this report a model based adaptive control strategy is suggested. The model used for controller design is based on ASM1. By applying some simplifying assumptions, a reduced order time varying state-space model is employed for describing the dynamic behavior of the nitrate in the anoxic compartment. The time varying model parameters are updated at each sampling period and estimated from measurements of nitrate concentration and Total Suspended Solids (TSS). The derived state-space model is then used in the design of a Linear Quadratic Gaussian (LQG) controller utilizing both feedback and feed-forward from measurable disturbances. The suggested control strategy can be regarded as an indirect adaptive LQG controller, which is described in [3]. The controller adapts to and compensates for changes in the system dynamics, since important system parameters are estimated adaptively. Another benefit with the suggested control strategy is that the estimated system parameters and states gives guidance about the state of the process and the characteristics of the wastewater.

2 Reduced Order State-Space Models for an Anoxic Compartment

The IAWQ activated sludge model No. 1 (ASM1) is a widely used model for simulation of the activated sludge process (ASP). The model includes 13 different components, and the dynamic behavior of each component is described by a nonlinear differential equation, see [13] and Appendix A). See also [5] and [8] for some general bioreactor models. Due to its large complexity, it is far from trivial to use the ASM1 directly for controller design or theoretical analysis of the system. In order to design model based controllers, reduced order state-space models of the ASM1 are derived in this section. The model reduction is based on lumping of components together with some simplifying assumptions, see also [15]. The procedure aims to maintain the basic mechanistic structure and the significant reactions in ASM1, while describing the system with a lower order model. Another reason for lumping components is that several of the components in ASM1 are not measurable. By lumping appropriate components, measurable variables may be obtained.

2.1 Derivation of a State-Space Model

Initially in the model reduction, one completely mixed anoxic compartment in a post-denitrifying system will be considered.

The following assumptions are introduced:

A2.1. The biological reactions in the compartment is described by ASMI and the compartment is completely mixed.

A2.2. The volume in the compartment is constant, V [m^3].

A2.3. The concentration of dissolved oxygen is zero, $S_O = 0$ [mg/l].

A2.4. The impact of an external carbon source is modeled as an addition of readily biodegradable substrate $S_S(t)$ [mg COD/l].

A2.5. The slowly biodegradable substrate, $X_S(t)$ [mg COD/l], is not included in the soluble COD (Chemical Oxygen Demand).

The dilution rate is $D(t) = Q(t)/V$, where $Q(t)$ is the time varying inflow to the compartment. The control signal is the diluted concentration, see also [23]:

$$u(t) = \frac{Q_c}{V} S_{S,C}(t) \tag{1}$$

where $Q_C(t)$ is the flow rate of the external carbon source and $S_{S,C}(t)$ [mg COD/l] is the COD concentration of the carbon source.

Assumptions **A2.1**, **A2.2** and **A2.4** result in that the dynamic behavior of the nitrate concentration, $S_{NO}(t)$, and the readily biodegradable substrate, $S_S(t)$, in a completely mixed anoxic reactor can be described by the mass balance:

$$\begin{aligned} \frac{dS_{NO}(t)}{dt} &= -R(t) + D(t)(S_{NO,in}(t) - S_{NO}(t)) && (2) \\ \frac{dS_S(t)}{dt} &= \alpha R(t) + D(t)(S_{S,in}(t) - S_S(t)) + H(t) + u(t) && (3) \end{aligned}$$

where the subscript in denotes the concentrations in the influent of the anoxic compartment. $H(t)$ is a hydrolysis term. Assumption **A2.3** implies that

$$\begin{aligned} R(t) &= \frac{1-Y_H}{2.86Y_H}\hat{\mu}_H\left(\frac{S_S(t)}{K_S + S_S(t)}\right)\left(\frac{S_{NO}(t)}{K_{NO} + S_{NO}(t)}\right)\eta_g X_{B,H}(t) && (4) \\ \alpha &= -\frac{2.86}{1-Y_H}, && (5) \end{aligned}$$

where Y_H is the yield of the heterotrophic biomass. The time varying concentrations and constant parameters are lumped into one unknown variable $R(t)$, which is the process rate term. For an explanation of the different parameters in (4)-(5) and their typical default values, see [13].

One difficulty in using the model (2)-(3) for control purposes is that $S_S(t)$, in general, is not directly measurable on-line. In practice, standard laboratory COD measurements on filtered samples of the wastewater is often considered to be equal to the amount of $S_S(t)$, see [15]. However, all soluble biodegradable matter is not necessarily readily biodegradable and moreover, particulate biodegradable matter may not be slowly biodegradable. Some guidelines for the determination of COD components is defined in [21], where it is proposed that the soluble COD should contain readily biodegradable substrate $S_S(t)$, soluble inert organic matter $S_I(t)$ and part of the slowly biodegradable substrate $X_S(t)$.

In order to obtain an appropriate state-space representation of the soluble COD, it is natural to define a new state variable as the sum of $S_S(t)$ and $S_I(t)$, especially if Assumption **A2.5** is taken under consideration. $S_I(t)$ is inert and therefore considered to be unaffected by biological reactions, i.e. the dynamics of $S_I(t)$ is modeled as $\dot{S}_I(t) = D(t)(S_{I,in}(t) - S_I(t))$. By introducing the new state variable $S_{COD}(t) = S_S(t) + S_I(t)$, the system (2)-(3) can be rewritten as:

$$\frac{dS_{NO}(t)}{dt} = -R(t) + D(t)(S_{NO,in}(t) - S_{NO}(t)) \tag{6}$$

$$\frac{dS_{COD}(t)}{dt} = \alpha R(t) + D(t)(S_{COD,in}(t) - S_{COD}(t)) + H(t) + u(t) \tag{7}$$

The complete process rate term in (4) is given by the relationship $R(t) = r_{S_S}(t)S_S(t)$, where

$$r_{S_S}(t) = \frac{1-Y_H}{2.86Y_H}\hat{\mu}_H\left(\frac{1}{K_S + S_S(t)}\right)\left(\frac{S_{NO}(t)}{K_{NO} + S_{NO}(t)}\right)\eta_g X_{B,H}(t).$$

Since $S_S(t)$ is hard to measure on-line, it is desirable to derive a corresponding relationship $R(t) = r_{S_{COD}}(t)S_{COD}(t)$, in order to formulate an observable and controllable state-space representation of the system (6)-(7). The fact that $S_S(t) = S_{COD}(t) - S_I(t)$, gives $R(t) = r_{S_S}(t)(S_{COD}(t) - S_I(t))$. A reasonable assumption is that $S_{COD} > 0$, and $r_{S_{COD}}(t)$ is then given by the identity:

$$R(t) = r_{S_S}(t)\frac{S_S(t)}{S_S(t) + S_I(t)}S_{COD}(t) = r_{S_{COD}}(t)S_{COD}(t). \tag{8}$$

The system (6)-(7) can now be rewritten as:

$$\frac{dS_{NO}(t)}{dt} = -r_{S_{COD}}(t)S_{COD}(t) + D(t)(S_{NO,in}(t) - S_{NO}(t)) \tag{9}$$

$$\begin{aligned}\frac{dS_{COD}(t)}{dt} &= \alpha r_{S_{COD}}(t)S_{COD}(t) + D(t)(S_{COD,in}(t) - S_{COD}(t)) \\ &+ H(t) + u(t)\end{aligned} \tag{10}$$

or:

$$\begin{aligned}\begin{bmatrix} \dot{S}_{NO}(t) \\ \dot{S}_{COD}(t) \end{bmatrix} &= \begin{bmatrix} -D(t) & -r_{S_{COD}}(t) \\ 0 & \alpha r_{S_{COD}}(t) - D(t) \end{bmatrix} \begin{bmatrix} S_{NO}(t) \\ S_{COD}(t) \end{bmatrix} + \begin{bmatrix} 0 \\ 1 \end{bmatrix} u(t) + \\ &+ \begin{bmatrix} 1 & 0 & 0 \\ 0 & 1 & 1 \end{bmatrix} \begin{bmatrix} D(t)S_{NO,in}(t) \\ D(t)S_{COD,in}(t) \\ H(t) \end{bmatrix}\end{aligned} \tag{11}$$

Considering $S_{NO}(t)$ as the output, the model (11) is controllable and observable if $r_{S_{COD}}(t) \neq 0$, see [28] for controllability and observability of time varying linear systems.

An extension of the model (11) to the case of two anoxic compartments is derived in Appendix D.

2.2 Derivation of an Augmented State-Space Model

A lot of research has been devoted to develop optical sensors that could replace the traditional laboratory COD measurements. However, today it is still not common to have on-line measurements of the soluble COD (S_{COD}) at wastewater treatment plants (WWTP's). One possibility to estimate soluble COD on-line may be to establish an empirical relationship between measurements of COD from filtered wastewater and measured TOC (Total Organic Carbon), see also [20].

In this section, the soluble COD will be estimated from on-line measurements which utilize sensors of more standard type. By lumping together unmeasurable ASM1 variables, new variables related to TSS (Total Suspended Solids) and total COD are obtained.

In order to obtain a measurable variable (see Remark **4.1** in Section 4), a new lumped variable is defined as:

$$X_{TSS}(t) = X_B(t) + X_I(t) + X_S(t), \tag{12}$$

where the total active biomass, $X_B(t)$, is the sum of heterotrophic and autotrophic biomass $X_B(t) = X_{B,H}(t) + X_{B,A}(t)$. The inert and particulate inert matter from biomass decay, as defined in ASM1, are combined into one matter $X_I(t)$. Another variable is defined as the sum of $X_{TSS}(t)$ and $S_{COD}(t)$:

$$X_{COD}(t) = X_{TSS}(t) + S_S(t) + S_I(t) = X_{TSS}(t) + S_{COD}(t). \tag{13}$$

$X_{COD}(t)$ can be regarded as the total COD. Summing up the reaction rates for the components in (12)-(13) (see Appendix A), the mass balance of the new variables (12)-(13) and the nitrate, $S_{NO}(t)$, can be written as:

$$\begin{aligned}
\frac{dS_{NO}(t)}{dt} &= -R(t) + D(t)(S_{NO,in}(t) - S_{NO}(t)) && (14)\\
\frac{dX_{TSS}(t)}{dt} &= -\alpha Y_H R(t) + D(t)(X_{TSS,in}(t) - X_{TSS}(t)) \\
&\quad - H(t) && (15)\\
\frac{dX_{COD}(t)}{dt} &= -2.86R(t) + D(t)(X_{COD,in}(t) - X_{COD}(t)) \\
&\quad + u(t) && (16)
\end{aligned}$$

Using (8), and exploiting the relationship $S_{COD}(t) = X_{COD}(t) - X_{TSS}(t)$ inserted in (8), the system (14)-(16) is obtained as:

$$\frac{dS_{NO}(t)}{dt} = -D(t)S_{NO}(t) + r_{S_{COD}}(t)X_{TSS}(t) - r_{S_{COD}}(t)X_{COD}(t) + D(t)S_{NO,in}(t) \tag{17}$$

$$\frac{dX_{TSS}(t)}{dt} = (\alpha Y_H r_{S_{COD}}(t) - D(t))X_{TSS}(t) - \alpha Y_H r_{S_{COD}}(t)X_{COD}(t) + D(t)X_{TSS,in}(t) - H(t) \tag{18}$$

$$\frac{dX_{COD}(t)}{dt} = 2.86 r_{S_{COD}}(t)X_{TSS}(t) - (2.86 r_{S_{COD}}(t) + D(t))X_{COD}(t) + D(t)X_{COD,in}(t) + u(t) \tag{19}$$

Using the relationship $X_{COD,in}(t) = X_{TSS,in} + S_{COD,in}$, a state-space representation of the system (17)-(19) can be written as:

$$\dot{z}(t) = \begin{bmatrix} -D(t) & r_{S_{COD}}(t) & -r_{S_{COD}}(t) \\ 0 & \alpha Y_H r_{S_{COD}}(t) - D(t) & -\alpha Y_H r_{S_{COD}}(t) \\ 0 & 2.86 r_{S_{COD}}(t) & -2.86 r_{S_{COD}}(t) - D(t) \end{bmatrix} z(t) + \begin{bmatrix} 0 \\ 0 \\ 1 \end{bmatrix} u(t) + \begin{bmatrix} 1 & 0 & 0 & 0 \\ 0 & 1 & -1 & 0 \\ 0 & 1 & 0 & 1 \end{bmatrix} \begin{bmatrix} D(t)S_{NO,in}(t) \\ D(t)X_{TSS,in}(t) \\ H(t) \\ D(t)S_{COD,in} \end{bmatrix} \tag{20}$$

where $z(t) = \begin{bmatrix} S_{NO}(t) & X_{TSS}(t) & X_{COD}(t) \end{bmatrix}^T$. The hydrolysis $H(t)$ and the influent soluble COD to the anoxic compartment, $S_{COD,in}$, may be regarded as non-measurable process disturbances. Note that the system (20) is not observable if $S_{NO}(t)$ is the only output. A minimal realization of (20) is simply the system (11), which is obtained by replacing the states $X_{COD}(t)$ and $X_{TSS}(t)$ with the new state variable $S_{COD}(t) = X_{COD}(t) - X_{TSS}(t)$. This will be exploited when designing the controllers in Section 4.

The system (20) is extended to two anoxic compartments in Appendix E.

2.3 Theoretical Identifiability

One important question is if the unknown parameter, $r_{S_{COD}}(t)$, in the suggested model (20) is theoretically identifiable. A simple method for investigating theoretical identifiability is the Taylor series expansion of observations method, see for example [15] and [8] for application on models for the ASP. Based on the analysis in Appendix B, the following result holds.

Conjecture 2.1 *The reaction rate term $r_{S_{COD}}(t)$ in (20), is theoretically identifiable under the following assumptions:*

A2.6. *$r_{S_{COD}}(t)$ and $D(t)$ are constants, i.e. not varying with time.*

A2.7. *The nitrate concentrations* $S_{NO,in}(t)$ *[mg/l] and* $S_{NO}(t)$ *[mg/l], are measurable.*

A2.8. *The concentrations of total suspended solids,* $X_{TSS,in}(t)$ *[mg COD/l] and* $X_{TSS}(t)$ *[mg COD/l] are measurable.*

A2.9. *The incoming soluble COD* ($S_{COD,in}$) *[mg COD/l] is measurable.*

Comment: Assumption **A2.9** is only temporary and will be somewhat relaxed in Section 5.2. Assumption **A2.6** is not true in practice and is only temporarily used in order to investigate the theoretical identifiability.

The Taylor series expansion of observations method can also be applied to (9)-(10). It is interesting to compare the identifiability results from (9)-(10) with the expression (30) in Appendix B. By investigating the theoretically identifiability of a constant $r_{S_{COD}}$ in the model (9)-(10), we can conclude that a constant $r_{S_{COD}}$ cannot be identified if $S_{COD}(t)$ is unmeasurable, since $r_{S_{COD}}(t)$ and $S_{COD}(t)$ always occur as a combined variable. Thus, the conclusion that can be drawn from the identifiability results is that in the case of unmeasurable $S_{COD}(t)$, a constant $r_{S_{COD}}$ can at least be theoretically identifiable using the model (20), if measurements of nitrate, TSS and $S_{COD,in}(t)$ are available and if $D(t)$ is a constant.

For the case when Y_H is unknown, the following conjecture based on the analysis in Appendix C, can be made.

Conjecture 2.2 *Consider the same assumptions as in Conjecture 2.1 and the following additional assumption:*

A2.10. *$H(t)$ is constant.*

The heterotrophic yield, Y_H, is then theoretically identifiable.

3 Estimation of the Reaction Rate Term

The transformed reaction rate term, $r_{S_{COD}}(t)$ appears in the models (11) and (20), derived in Section 2. Since $r_{S_{COD}}(t)$ is unknown, it has to be estimated in an appropriate way. One approach is to approximate the reaction rate term as constant, which gives the possibility to use off-line estimation techniques. With an additional assumption that $D(t)$ is constant, the system matrices in (11) and (20) will be time invariant, which simplifies the control synthesis. One drawback with this approach is that if the assumption regarding the constant reaction rate term is inexact, important information about the system dynamics may be lost.

In this section, the reaction rate term will be estimated on-line. Allowing $r_{S_{COD}}(t)$ to be time varying implies the possibility for the models to adapt to important system dynamics. The time varying reaction rate term also gives guidance about the state of the process. $r_{S_{COD}}(t)$ will be estimated from (20) with an Extended Kalman Filter (EKF).

3.1 Estimation of the Reaction Rate Term with known Heterotrophic Yield, Y_H

In this section one anoxic compartment is considered and it is assumed that the yield of the heterotrophic biomass, Y_H, is known in the model (20).

In order to use an EKF discrete-time algorithm, the model (20) can be sampled and augmented according to the following steps:

1. The model (20) is sampled which gives the discrete-time system:

$$z(t+1) = A_s(t)z(t) + B_H(t)H(t) + B_u(t)u(t) + B_m(t)m(t), \qquad (21)$$

   where $m(t)^T = D(t)[S_{NO,in}(t) \;\; X_{TSS,in}(t) \;\; S_{COD,in}(t)]$ are measurable disturbances. A zero-order hold sampling is used, see e.g. [4].

2. In order to obtain the Jacobian matrix in the EKF-algorithm (see Appendix F) the model (20) is linearized with respect to $z(t)$ and $r_{S_{COD}}(t)$ and then sampled.

3. Next, the unknown parameters $H(t)$ and $r_{S_{COD}}(t)$ are modeled as AR-processes:

$$
\begin{aligned}
r_{S_{COD}}(t+1) &= \phi r_{S_{COD}}(t) + e(t) \\
H(t+1) &= \phi H(t) + v(t),
\end{aligned} \tag{22}
$$

where $e(t)$ and $v(t)$ are white noise. A choice $\phi = 1$ would correspond to a random walk process. In what follows, we will choose $\phi = 0.99$, which can be seen as a filtered random walk.

4. The system (21) is then augmented with $H(t)$ and $r_{S_{COD}}(t)$ as additional states:

$$
\begin{aligned}
\begin{bmatrix} z(t+1) \\ r_{COD}(t+1) \\ H(t+1) \end{bmatrix} &= \begin{bmatrix} A_s(t) & 0 & B_H(t) \\ 0 & 0.99I & 0 \\ 0 & 0 & 0.99I \end{bmatrix} \begin{bmatrix} z(t) \\ r_{COD}(t) \\ H(t) \end{bmatrix} \\
&+ \begin{bmatrix} B_u(t) \\ 0 \\ 0 \end{bmatrix} u(t) + \begin{bmatrix} B_m(t) \\ 0 \\ 0 \end{bmatrix} m(t) + \begin{bmatrix} 0 & 0 \\ I & 0 \\ 0 & I \end{bmatrix} \begin{bmatrix} e(t) \\ v(t) \end{bmatrix}.
\end{aligned} \tag{23}
$$

5. By augmenting the Jacobian matrix in the same manner as in step 4, the hydrolysis, $H(t)$, the reaction rate term, $r_{S_{COD}}(t)$, and the unmeasurable state, $X_{COD}(t)$, can now be updated using one step in the discrete-time EKF algorithm. After updating the model (20) with the new estimates, the procedure is repeated.

See Appendix F for a summarized discrete-time EKF algorithm. Another approach is to use a continuous-discrete EKF, which has the benefit to keep the model in the continuous form, while the measurements are discrete in time. For more practical aspects of extended Kalman filtering, see [11]. The estimation of the unknown states, the reaction rate terms and the hydrolysis terms for two anoxic compartments is illustrated by simulations in Section 5.2.

3.2 Estimation of the Heterotrophic Yield, Y_H

In Section 3.1, the heterotrophic yield, Y_H, was assumed to be known. Y_H can be determined using respirometry by addition of an amount of wastewater COD and measurements of the substrate oxidation , see e.g. [25] and [21]. Y_H will be estimated on-line from measurements of $S_{NO}(t)$ and $X_{TSS}(t)$ using a discrete-time EKF. A related strategy can be found in [22] where Y_H and the hydrolysis in one anoxic compartment is estimated from measurements of $S_{NO}(t)$ and $S_S(t)$ using a Kalman filter.

Let the parameter β be defined as $\beta = \alpha Y_H$. The heterotrophic yield is then obtained from $Y_H = \frac{\beta}{\beta - 2.86}$ using (3). The unknown parameter β is modeled as an AR-process, see (22), and the state vector in (23) is augmented with the new state β. The unknown states can be estimated in the same way as in Section 3.1 using a discrete-time EKF. Here, the tracking problem involves simultaneous estimation of the four unknown parameters β, $r_{S_{COD}}(t)$, $H(t)$ and $X_{COD}(t)$. The estimation of the heterotrophic yield, reaction rate terms and the hydrolysis terms, for two anoxic compartments is illustrated by simulations in Section 5.4.

4 Controller Design

In this section the case of two anoxic compartments is considered. The components in the first and second compartment are denoted by the subscripts 1 and 2 respectively. The LQG controller design is based on the two models (32) and (38) in Appendix D and Appendix E. The augmented state-space model (38) is used for the estimation part. If $D(t)$ and $r_{S_{COD,i}}(t) \neq 0$, $i = 1,\ 2$, are assumed to be constants, the model (32) is a minimal realization, which is not the case for the model (38). Therefore, the controller design is based on model (32).

The assumptions (**A2.7**)-(**A2.9**) in Section 2.3 are used. However, **A2.7** and **A2.8** are modified to hold for two anoxic compartments, and **A2.9** is somewhat relieved in order to hold for measurement methods of standard type:

A4.1. The nitrate concentrations, $S_{NO,in}(t)$ [mg/l] and $S_{NO,2}(t)$ [mg/l], are measurable.

A4.2. The concentrations of total suspended solids, $X_{TSS,in}(t)$ [mg COD/l], $X_{TSS,1}(t)$ [mg COD/l] and $X_{TSS,2}(t)$ [mg COD/l] are measurable.

A4.3. The incoming soluble COD ($S_{COD,in}$) [mg COD/l] is measured in twenty-four hour intervals from laboratory tests.

Remark 4.1. In practice, insoluble particles can be measured on-line using, for example, turbidimeters. Turbidity is related to the content of suspended solids (SS) and there are also laboratory tests for solids that can calibrate turbidity measurements, see [20]. However, insoluble particles also contains other materials than organic particles. It is also necessary to convert the measurement of TSS to have the same unit as $X_{TSS}(t)$. A survey of new and existing technologies for measuring different components and variables in wastewater, including SS, is presented in [26].

The LQG controller will be designed in discrete-time. Hence, the first step is to sample the system (32) using zero-order hold sampling. In order to obtain a feedforward action in the LQG controller, the measurable disturbance $d(t)$ from (33) is included in the state vector in (32). The dynamics of $d(t)$ is modeled as an AR-process, see (22) in Section 3.1. Several different strategies for how to design an integrating controller exist. The approach used here is based on differentiating the system and deriving an incremental controller, see e.g. [10].

After rewriting (32) in a discrete and differential form, with $d(t)$ included in the state vector, a feedforward-feedback integrating LQG controller can be designed. The differentiation of the model results in the disappearance of constant process disturbances in the model. To see this, assume that:

A4.4. The hydrolysis terms $H_i(t)$ are slowly time varying.

This will result in that $H_i(t)$ can be omitted from (32) when deriving the LQG controller. The sampled and differentiated system can now be written as, see further ([16]):

$$\begin{bmatrix} \Delta x_n(t+1) \\ y(t+1) \end{bmatrix} = A_d(t) \begin{bmatrix} \Delta x_n(t) \\ y(t) \end{bmatrix} + B_d(t)\Delta u(t) \tag{24}$$

where $A_d(t)$ and $B_d(t)$ are the discrete-time system matrices obtained from sampling and differentiating (32), and $y(t) = S_{NO,2}(t)$ is the output signal. Further, $\Delta x_n(t+1) = x_n(t+1) - x_n(t)$ and so on. The differentiated state vector is $\Delta x_n(t) = \begin{bmatrix} \Delta x(t) & \Delta d(t) \end{bmatrix}^T$, where

$$\Delta x(t) = \begin{bmatrix} \Delta S_{NO,1}(t) & \Delta S_{NO,2}(t) & \Delta S_{COD,1}(t) & \Delta S_{COD,2}(t) \end{bmatrix}^T,$$

and the differentiated control signal can then be computed as

$$\begin{aligned} \Delta u(t) &= -L \begin{bmatrix} \Delta \hat{x}_n(t) \\ y(t) \end{bmatrix} + L_w w(t) = \\ &- \begin{bmatrix} L_{x_n} & L_y \end{bmatrix} \begin{bmatrix} \Delta \hat{x}_n(t) \\ y(t) \end{bmatrix} + L_w w(t) \end{aligned} \tag{25}$$

where $w(t)$ is the reference signal (set-point of the nitrate). A suitable choice of L_w is $L_w = L_y$, because the set-point $w(t)$ and output $y(t)$ are then amplified equally. The state feedback (and disturbance feedforward) vector L is found by minimizing the cost function:

$$\lim_{n\to\infty} \sum_{t=1}^{n} \left(\begin{bmatrix} \Delta x_n(t) \\ y(t) \end{bmatrix}^T Q_1 \begin{bmatrix} \Delta x_n(t) \\ y(t) \end{bmatrix} + \Delta u(t)^T Q_2 \Delta u(t) \right) \tag{26}$$

where Q_1 and Q_2 are positive definite penalty matrices, see also, e.g. [4].

An EKF observer is used for estimating the unmeasurable states in $\Delta x(t)$ and the reaction rate terms, $r_{S_{COD,i}}(t)$, in (32). After zero-order hold sampling, the model (38) is augmented with the reaction rate terms and the hydrolysis terms H_i. The soluble COD in the two compartments can now be estimated using the relationship, $\hat{S}_{COD,i}(t) = \hat{X}_{COD,i}(t) - X_{TSS,i}(t)$, where $\hat{X}_{COD,i}(t)$ is estimated by the EKF. The system matrices, A_d and B_d, in (24) are updated at each sampling instant using the EKF estimates of $\hat{r}_{S_{COD,i}}(t)$.

The controller design in this section can be regarded as an indirect adaptive LQG controller, which is illustrated in Figure 1. A recursive least squares (RLS) estimation procedure has also been evaluated, but recent results indicate that the EKF performs better.

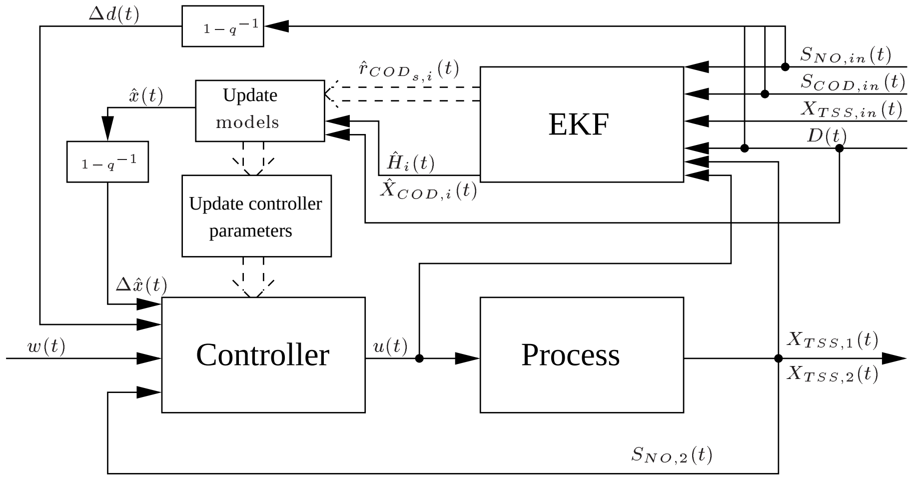

Figure 1: Block diagram of the adaptive LQG controller with EKF.

5 Simulation Studies

5.1 Simulation Set Up

The feedback-feedforward adaptive LQG control law given by (25) was studied on the ASM1 in a post-denitrifying ASP. The simulated ASP consisted of eight aerobic compartments, two anoxic compartments and one settler. Matlab was used to implement the model. The parameters in the model were the default values given in [13]. The total volume of the plant was $6000m^3$. Each anoxic compartment had the volume $V_{anox} = 1000m^3$, and each aerobic compartment had the volume $V_{aerobic} = 500m^3$. The excess sludge flow rate was $Q_w = 16m^3/h$. The plant was simulated using influent data from the file dryinfluent.mat and storminfluent.mat from the COST benchmark, see htpp://www.ensic.unancy.fr/COSTWWTP/ and [1].

In the tuning of the controller parameters, influent data were taken from the file dryinfluent.mat. A traditional PI controller was used for controlling the level of dissolved oxygen (DO) in the aerobic compartments, and the DO set-point was chosen to be $2mg/l$ in each compartment. The return sludge flow rate was controlled so that a constant ratio between the return sludge flow rate and the influent flow rate was obtained.

5.2 Simulations Using an LQG Controller assuming Y_H known

In this section the assumptions (**A4.1**)-(**A4.3**) are used. $S_{NO,1}(t)$, $X_{COD,1}(t)$ and $X_{COD,2}(t)$ were estimated using an EKF and $S_{COD,i}(t)$ was estimated as, $\hat{S}_{COD,i}(t) = \hat{X}_{COD,i}(t) - X_{TSS,i}(t)$. The data used for estimation and control were sampled with a sampling period of 1 minute without noise and delay on the sensors.

The external carbon source was assumed to be ethanol with $S_{S,C} = 1200000$ mg (COD)/l. An upper bound on the external carbon flow rate was introduced and chosen as 5 m^3 ethanol/day. The design variables in the LQG controller were chosen in a way so that the controller behaved as fast as possible without exceeding the upper bound on $u(t)$ when influent data from the file dryinfluent.mat was used. The nitrate set-point was $4mg/l$. For the LQG controller the penalty matrices in (26) were chosen as $Q_1 = diag[0, 0, 0, 0, 1, 1, 1]$ and $Q_2 = 25000$. The initial value of the covariance matrix in the EKF was chosen as $P(0) = I$, where I denotes the unity matrix, and the design variables as $R_1 = diag[10, 1, 10, 1, 1, 1, 1, 1, 1, 0.01]$ and $R_2 = 0.01I$, see Appendix F.

For comparison, a traditional PID controller and a PI controller with feedforward [23] were also implemented. The feedforward part uses measurements of the influent $S_S(t)$ of the first anoxic compartment. The control parameters in the traditional PID controller and the PI controller with feedforward were tuned to make the controllers as fast as possible without exceeding the upper bound on $u(t)$, when simulating using influent data from the file dryinfluent.mat. The upper bound on $u(t)$ and the nitrate set-point were the same as for the LQG controller. It is worth noticing that none of the controllers are optimally tuned.

5.2.1 Results and Discussion

The simulation results for the three different controllers are illustrated in Figure 2. The seven last days of the simulations using influent data from the storminfluent.mat file are shown in the plots. By comparing the LQG controller and a traditional PID controller without feedforward, it is seen that the LQG controller gives a faster disturbance rejection than the PID controller. The PI controller with feedforward, in the same figure, has a similar performance as the LQG controller. During the larger disturbances at day 2 and 4 the controllers reach the upper bound on $u(t)$. The total consumption of external carbon during the period, (u_{cons}), and the variance of the control error, (e_{var}), for the three controllers are shown in Table 1.

Notice that the PI controller with feedforward uses measurements of both $S_{NO,in}(t)$ and $S_{S,in}(t)$. Previous work where the LQG design and the esti-

Table 1: The variance of the control error, (e_{var}), and the total consumption of external carbon during the period, (u_{cons}), for the three controllers.

Controller	e_{var}	u_{cons}
LQG	0.468	16.17
PI-feedforward	0.440	16.41
PID	1.175	16.37

mation procedure is based on on-line measurements of $S_{COD}(t)$ has shown that the LQG controller gives faster disturbance rejection than the PI controller with feedforward, see [9]. However, one drawback with the LQG design is the implementation part, which is more complex compared to the PI controller with feedforward.

Figure 3 illustrates the EKF estimation of $r_{S_{COD,1}}(t)$ and $r_{S_{COD,2}}(t)$. The EKF also provides a good estimate of the total COD and satisfactory estimates of the hydrolysis terms in both anoxic compartments. The convergence of the estimates of $r_{S_{COD,i}}(t)$ and $H_i(t)$ is improved with the reasonable assumption **A4.3**. Figure 4 and 5 illustrate the estimates of $X_{COD,i}(t)$ and $H_i(t)$, respectively. All fourteen days from the storminfluent.mat file are shown in the plots.

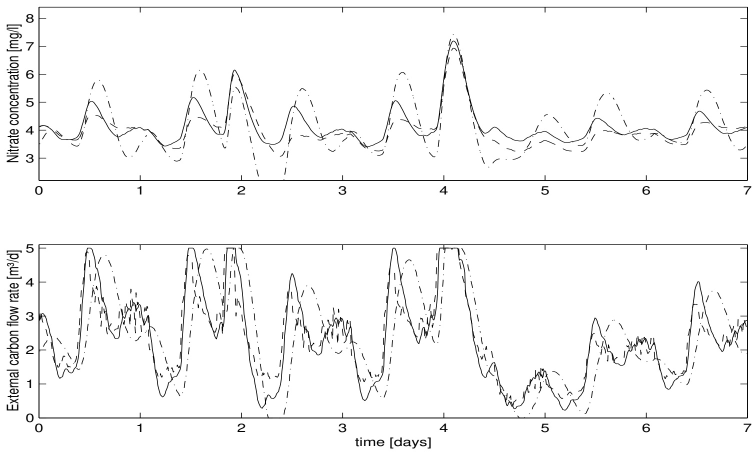

Figure 2: Upper plot: The solid line shows the nitrate concentration in the last anoxic compartment when the LQG controller is used, dashed line the nitrate concentration when PI with feedforward is used, and dashed-dotted line the nitrate concentration when a traditional PID controller is used. Lower plot: The external carbon flow rates are shown for the three controllers, respectively.

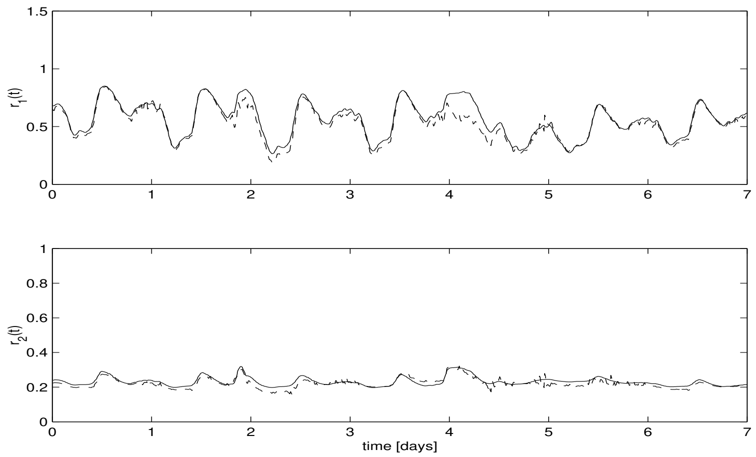

Figure 3: Upper plot: The dashed line shows the EKF estimated value of the reaction rate term $r_{S_{COD,1}}(t)$ and the solid line the true value. Lower plot: The dashed line shows the EKF estimated value of the reaction rate term $r_{S_{COD,2}}(t)$ and the solid line the true value.

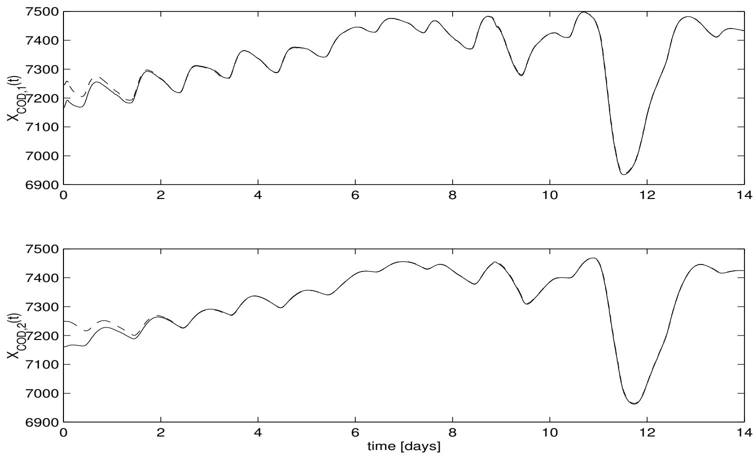

Figure 4: Upper plot: The dashed line shows the EKF estimated value of $X_{COD,1}(t)$ and the solid line the true value of $X_{COD,1}(t)$. Lower plot: The dashed line shows the EKF estimated value of $X_{COD,2}(t)$ and the solid line the true value of $X_{COD,2}(t)$.

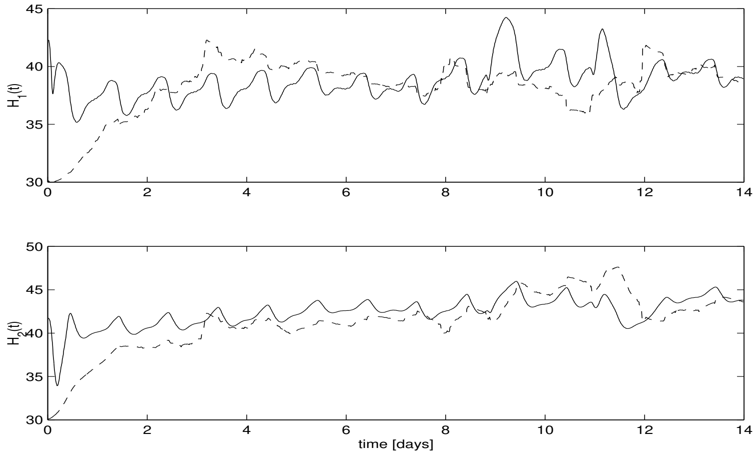

Figure 5: Upper plot: The dashed line shows the EKF estimated value of the hydrolysis term $H_1(t)$ and the solid line the true value. Lower plot: The dashed line shows the EKF estimated value of the hydrolysis term $H_2(t)$ and the solid line the true value.

5.3 Estimating the Reaction Rate Terms, $r_{S_{COD,1}}(t)$ and $r_{S_{COD,2}}(t)$, during Toxic Load Event

In order to investigate the performance of the EKF estimates of $r_{S_{COD,1}}(t)$ and $r_{S_{COD,2}}(t)$ during abnormal conditions, a toxic load event was simulated using the dryinfluent.mat file. It was assumed that the toxic load results in an increased decay of microorganisms and a decrease of the specific growth rate. The process conditions are changed more drastically in the aerobic compartments, since the nitrifying bacteria are generally more sensitive to toxic compounds than other bacteria.

The same LQG controller as in Section 5.2 was used in the simulation. After day one, the decay rate coefficient, b_a, for autotrophic biomass is suddenly increased with 60 % and the decay rate coefficient, b_h, for heterotrophic biomass is increased with 30 %. At the same event, the maximum specific growth rate for autotrophic biomass is decreased with 50 % and the maximum specific growth rate for heterotrophic biomass decreased with 30 %. This may simulate the behavior of the plant when a toxic compound suddenly appears in the wastewater. The coefficients are thereafter changed stepwise back to normal values, and after 8.3 days the biological properties of the microorganisms are recovered to normal conditions.

5.3.1 Results and Discussion

Figure 6 illustrates the EKF estimation of $r_{S_{COD,1}}(t)$ and $r_{S_{COD,2}}(t)$. It is seen that especially $r_{S_{COD,2}}(t)$ is difficult to estimate during the toxic load event. The explanation is probably a too poor excitation of the input signal, since the external carbon flow rate, $u(t)$, is zero during long periods. However, the result shows that at least the estimate of $r_{S_{COD,1}}(t)$ may be used as a toxic load indicator.

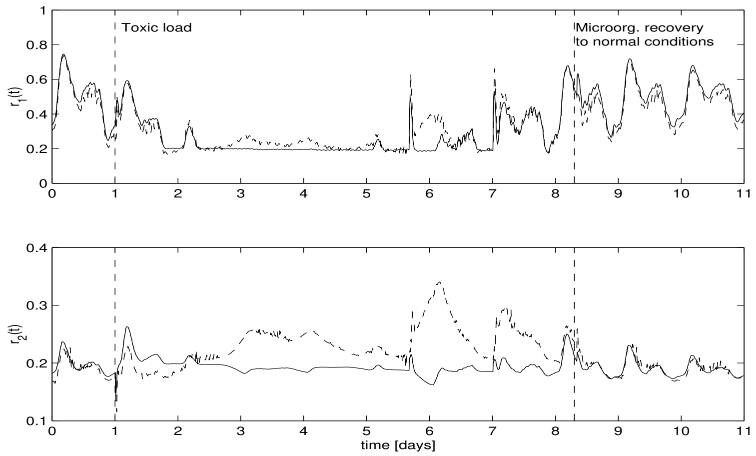

Figure 6: Upper plot: The dashed line shows the EKF estimated value of the reaction rate term $r_{S_{COD,1}}(t)$ and the solid line the true value. Lower plot: The dashed line shows the EKF estimated value of the reaction rate term $r_{S_{COD,2}}(t)$ and the solid line the true value.

5.4 Estimation of Y_H

As in Section 5.2, the assumptions (**A4.1**)-(**A4.3**) are used. In order to make the estimation procedure simpler, it was also assumed that the nitrate in the first anoxic compartment, $S_{NO,1}(t)$, was measured. An LQG controller was used simultaneously with the estimation of the unknown parameters, in order to control the nitrate concentration in the last anoxic compartment. In the estimation, influent data were taken from the file dryinfluent.mat. The data used for estimation were sampled with an interval of 1 minute without delay on the sensors. However, measurement noise with a standard deviation of 0.1 was added to the nitrate concentrations $S_{NO,1}(t)$, $S_{NO,2}(t)$ and $S_{NO,in}(t)$ and with a standard deviation of 0.05 to the SS concentrations $X_{TSS,1}(t)$, $X_{TSS,2}(t)$ and $X_{TSS,in}(t)$.

The initial value of the covariance matrix in the EKF was chosen as $P(0) = diag[1, 1, 1, 1, 1, 1, 5, 5, 10, 50, 50]$, and the design variables as
$R_1 = diag[1, 1, 1, 1, 1, 1, 0.05, 0.05, 0.001, 3, 3]$ and $R_2 = 0.01I$. The initial value for the state vector was $[8, 6, 7200, 7200, 7250, 7250, 1, 0.53, 10, 10]^T$.

5.4.1 Results and Discussion

Figure 7 shows the external carbon flow rate generated by the LQG controller during the simulation. This is the input used to excite the system. Figure 8 illustrates the EKF estimation of Y_H. Although the convergence is fairly slow, it is seen from the plot that the estimate of Y_H comes fairly close to the true value. The estimation performance, especially for the hydrolysis terms and Y_H, seems to be rather dependent on the choice of design variables R_1, R_2, and $P(0)$, and the design variables can only be chosen in a small range to avoid biased estimates. Figure 9 shows that the EKF provides good estimates of the reaction rate terms and Figure 10 illustrates a satisfactory estimates of the hydrolysis terms.

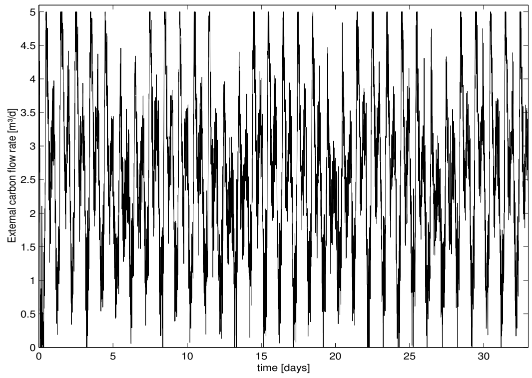

Figure 7: The input signal (external carbon flow rate generated by the LQG controller) used to excite the system.

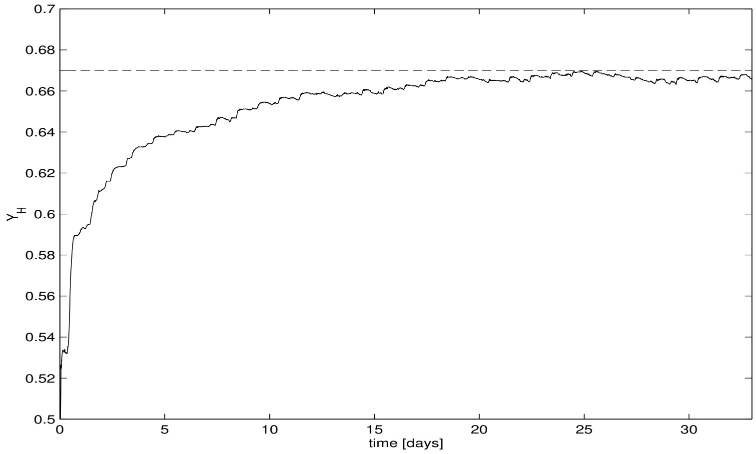

Figure 8: Simulations performed with a measurement noise with standard deviation 0.1 on the nitrate sensors, and with a measurement noise with standard deviation 0.05 on the SS sensors. Solid line shows the value of Y_H estimated with the EKF. Dashed line shows the true value.

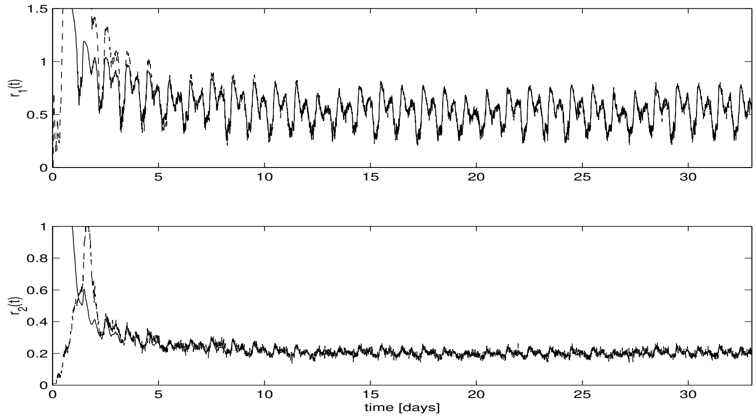

Figure 9: Simulations performed with a measurement noise with standard deviation 0.1 on the nitrate sensors, and with a measurement noise with standard deviation 0.05 on the SS sensors. Upper plot: The dashed line shows the EKF estimated value of the reaction rate term $r_{S_{COD,1}}(t)$ and the solid line the true value. Lower plot: The dashed line shows the EKF estimated value of the reaction rate term $r_{S_{COD,2}}(t)$ and the solid line the true value.

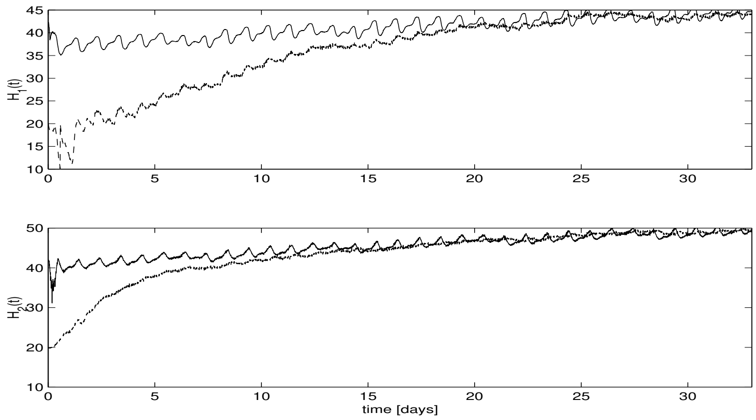

Figure 10: Simulations performed with a measurement noise with standard deviation 0.1 on the nitrate sensors, and with a measurement noise with standard deviation 0.05 on the SS sensors. Upper plot: The dashed line shows the EKF estimated value of the hydrolysis term $H_1(t)$ and the solid line the true value. Lower plot: The dashed line shows the EKF estimated value of the hydrolysis term $H_2(t)$ and the solid line the true value.

6 Conclusions

In this report, a model based control strategy for control of the nitrate level in the last anoxic compartment, using an external carbon source is presented. By lumping some states in ASM1, a feasible state space model for estimation was derived. The model was then used for on-line design of an integrating LQG controller. This strategy can be regarded as an indirect adaptive LQG control. The controller was evaluated in a simulation study and performed well despite major process disturbances. In the EKF estimation procedure, it is possible to use sensors of more standard type. Interesting topics for further research is to extend the controller for internal flow rate control and supervisory dissolved oxygen control. Also an evaluation using pilot or full scale experiments could be done. The strategy for estimating the reaction rate terms may also be further improved.

Acknowledgments

The financial support by the MISTRA program Sustainable Urban Water Management is gratefully acknowledged.

References

[1] J. Alex, J. Beteau, C. Hellings, U. Jeppsson, S. Marsili-Libelli, M. Pons, H. Spanjers, and H. Vanhooren. Benchmark for evaluating control strategies in wastewater treatment plants. In *Proc. of the European Control Conference, ECC99'*, 1999. Karlsruhe, Germany.

[2] H. Aspegren, U. Nyberg, J. Jansen, and B. Andersson. Model and sensor based optimization of nitrogen removal at the Klagshamn wastewater treatment plant. *Wat. Sci. Tech.*, 26(5–6):1315 – 1323, 1992.

[3] K. J. Åström and B. Wittenmark. *Adaptive Control*. Addison-Wesley, 1989.

[4] K. J. Åström and B. Wittenmark. *Computer-Controlled Systems*. Prentice-Hall International Editions, New Jersey, 1990.

[5] G. Bastin and D. Dochain. *On-line Estimation and Adaptive Control of Bioreactors*. Elsevier, Amsterdam, 1990.

[6] B. Carlsson and R. Milocco. A simple stratgy for controlling the nitrate concentration in an activated sludge process using external carbon flow rate. *Latin American Applied Research*, 31(2):115–120, 2001.

[7] J. Cho, S. Sung, and I. Lee. Cascade control strategy for external carbon dosage in predenitrifying process. *Wat. Sci. Tech.*, 45(4-5):53–60, 2002.

[8] D. Dochain and P. A. Vanrolleghem. *Dynamical Modelling and Estimation in Wastewater Treatment Processes*. IWA Publishing, 2001.

[9] M. Ekman, P. Samuelsson, and B. Carlsson. Adaptive control of the external carbon flow rate in an activated sludge process. In *1st World Water Congress of the IWA. Melbourne*, 2002. Poster presentation.

[10] C. E. García, D. M. Prett, and M. Morari. Model predictive control: Theory and practice – a survey. *Automatica*, 25(3):335–348, 1989.

[11] A. Gelb. *Applied Optimal Estimation*. MIT Press, Cambridge, MA, 1975.

[12] S. Hallin and M. Pell. Denitrification in activated sludge with external carbon sources - perspectives and consequences. *Vatten*, 53(3):213–216, 1996. In Swedish.

[13] M. Henze, C. P. L. Grady Jr., W. Gujer, G. v. R. Marais, and T. Matsuo. Activated sludge model no. 1. Scientific and Technical Report No. 1, 1987. IAWPRC, London.

[14] M. Henze, P. Harremoës, J. Jansen, and E. Arvin. *Wastewater Treatment, Biological and Chemical Processes*. Springer-Verlag, Berlin Heidelberg, Germany, 1995.

[15] U. Jeppsson. *Modelling aspects of wastewater treatment processes.* PhD thesis, Dept. of Industrial Electrical Eng. and Automation. Lund Institute of Technology, 1996. ISBN 91-88934-00-4; CODEN:LUTEDX/(TEIE-1010)/1-444/(1996).

[16] C.-F. Lindberg. *Control and Estimation Strategies Applied to the Activated Sludge Process.* PhD thesis, Systems and Control Group, Uppsala University, 1997.

[17] C.-F. Lindberg and B. Carlsson. Adaptive control of external carbon dosage in an activated sludge process. *Wat. Sci. Tech.*, 34(3–4):173–180, 1996.

[18] L. Lukasse. *Control and identification in activated sludge processes.* PhD thesis, Landbouwuniversiteit, Wageningen, 1999. ISBN 90-5485-956-3.

[19] L. Lukasse, K. Keesman, and G. van. Straten. Identification for model predective control of biotechnological processes, case study: nitrogen removal in an activated sludge process. In *Proceedings IFAC SYSID '97*, volume 3, pages 1525–1530, 1997.

[20] G. Olsson and B. Newell. *Wastewater Treatment Systems.* IWA Publishing, 1999.

[21] B. Petersen. *Calibration, identifiability and optimal experimental design of activated sludge models.* PhD thesis, Universiteit Gent, 2000.

[22] P. Samuelsson. *Modelling and control of activated sludge processes with nitrogen removal.* Licentiate thesis, Uppsala University, Systems and Control Group, 2001.

[23] P. Samuelsson and B. Carlsson. Feedforward control of the external carbon flow rate in an activated sludge process. *Wat. Sci. Tech*, 43(1):115–122, 2001.

[24] T. Söderström. *Discrete-Time Stochastic Systems.* Prentice Hall International, Hemel Hempstead, UK, 1994.

[25] U. Sollfrank and W. Gujer. Characterisation of domestic wastewater for mathematical modelling of the activated sludge process. *Wat. Sci. Tech.*, 23:1057 – 1066, 1991.

[26] P. A. Vanrolleghem and D. S. Lee. On-line monitoring equipment for wastewater treatment processes: State of the art. *Wat. Sci. Tech.*, 47(2):1 – 34, 2003.

[27] S. Weijers. *Modelling, identification and control of activated sludge plants for nitrogen removal.* PhD thesis, Technische Universiteit, Eindhoven, 2000.

[28] J. R. Wilson. *Linear Systems Theory.* Prentice Hall, New Jersey, 1993.

[29] Z. Yuan, H. Bogaert, P. Vanrolleghem, C. Thoeye, G. Vansteenkiste, and W. Verstraete. Control of external carbon addition to predenitrifying systems. *Environmental Engineering*, 123(11):1080–1086, 1997.

Recent technical reports from the Department of Information Technology

2003-011 Alexandre David, Gerd Behrmann, Kim G. Larsen, and Wang Yi: *A Tool Architecture for the Next Generation of UPPAAL*

2003-012 Ken Mattsson and Jan Nordström: *Finite Difference Approximations of Second Derivatives on Summation by Parts Form*

2003-013 Ken Mattsson, Magnus Svärd, and Jan Nordström: *Stable Artificial Dissipation Operators for High Order Finite Difference Schemes*

2003-014 Brahim Hnich, Julian Richardson, and Pierre Flener: *Towards Automatic Generation and Evaluation of Implied Constraints*

2003-015 Henrik Björklund and Sven Sandberg: *Algorithms for Combinatorial Optimization and Games Adapted from Linear Programming*

2003-016 Bertil Gustafsson and Eva Mossberg: *Time Compact High Order Difference Methods for Wave Propagation*

2003-017 Henrik Björklund, Sven Sandberg, and Sergei Vorobyov: *An Improved Subexponential Algorithm for Parity Games*

2003-018 Magnus Svärd, Ken Mattsson, and Jan Nordström: *Steady State Computations Using Summation-by-Parts Operators*

2003-019 Henrik Björklund, Sven Sandberg, and Sergei Vorobyov: *Randomized Subexponential Algorithms for Parity Games*

2003-020 Christian Tschudin and Richard Gold: *SelNet: A Translating Underlay Network*

2003-021 Christian Tschudin and Richard Gold: *LUNAR: Lightweight Underlay Network Ad-hoc Routing*

2003-022 Bharath Bhikkaji, Kaushik Mahata, and Torsten Söderström: *Reduced order models for a two-dimensional heat diffusion system*

2003-023 Bertil Gustafsson and Per Wahlund: *Time Compact Difference Methods for Wave Propagation in Discontinuous Media*

2003-024 Parosh Aziz Abdulla, Bengt Jonsson, Marcus Nilsson, and Julien d'Orso: *Algorithmic Improvements in Regular Model Checking*

2003-025 Torbjörn Wigren and Torsten Söderström: *Second Order ODEs are Sufficient for Modeling of Many Periodic Signals*

2003-026 Henrik Löf, Zoran Radovic, and Erik Hagersten: *THROOM — Running POSIX Multithreaded Binaries on a Cluster*

2003-027 Per Carlsson, Arne Andersson, and Fredrik Ygge: *A Tractable Mechanism for Time Dependent Markets*

2003-028 Erik K. Larsson: *Limiting Properties of Sampled Stochastic Systems*

2003-029 Oskar Grenholm, Zoran Radovic, and Erik Hagersten: *Latency-hiding and Optimizations of the DSZOOM Instrumentation System*

2003-030 M. Ekman, P. Samuelsson, and B. Carlsson: *Adaptive Control of the Nitrate Level in an Activated Sludge Process Using an External Carbon Source - Extended Version*

UPPSALA
UNIVERSITET

May 2003
ISSN 1404-3203
http://www.it.uu.se/